THIN FOIL PHYSICAL EFFECTS ON THE TRANSPORT OF AN INTENSE RELATIVISTIC ELECTRON BEAM

O. Mouton, D. Guilhem, CEA/DIF/DPTA/SPAA, BP12, 91680 Bruyères-le-Châtel, FRANCE

Abstract

In an AIRIX like accelerator facility, debris of the target are ejected when the electron beam impacts the X conversion target. A rotating mechanical device choking periodically the vacuum chamber but allowing the electron beam to pass through when it is correctly synchronized, is usually implemented to preserve the accelerating gaps from pollution. We looked into the feasability of another solution consisting of a thin metallic foil which could be crossed by the beam without beeing dammaged. While it crosses a perpendicular thin foil, an electron beam suffers not only a well known emittance growth due to the Coulomb scattering effect but also an additional electromagnetic focusing effect. The propagation of the beam is then modified by these perturbations. In beam dynamic simulations, the foil has to be taken into account in addition, as a thin non linear lens. In this paper we compare the last experimental results carried on the PIVAIR accelerator end (EOA) to the beam envelope simulations obtained with the TRAJENV code.

1 FOIL EXPERIMENTS

The PIVAIR facility [1] delivers a 6 MeV, 3 kA, 60 ns electron beam. In 1999 and 2000, several experiments were carried out. The EOA consisted mainly of two focusing solenoids, steering coils, a vacuum pumping module, beam diagnostics, a metallic foil and a final target (see fig. 1).

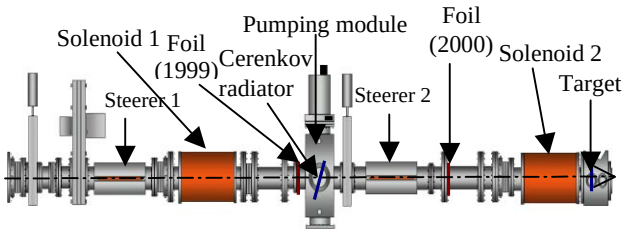

Figure 1 : Accelerator end showing the two solenoid lenses and the foil locations.

1.1 Physical effects of a conducting foil

Different kinds of foils (aluminum, grid) have been mounted in the vacuum chamber perpendicularly to the z-axis ahead of the pumping module (fig.1). The mechanical holding is shown on figure 2.

For different values of the solenoid lens #1 current, the radii of the beam were measured 11 cm ahead of the foil , thanks to a Cerenkov radiator (fig. 3). In all cases, the decrease of the beam radius versus the solenoid current is due to the stronger focusing action of the solenoidal magnetic field. We take as a reference case (a) the first result without foil or grid. Case (b) corresponds to a grid in place of the foil. In comparison to the reference case, the focusing effect from the grid is clearly seen.

Figure 2 : Foil holder

If now a 15 µm thick foil replaces the grid (c), the beam size slightly increases. This differential behavour is due to the electron scattering in the foil. As expected, this effect is enhanced for a thicker foil (100µm) (d).

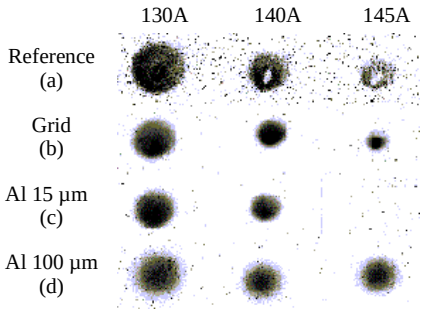

Figure 3 : Cerenkov images for three solenoid currents , reference (a), effect of a a grid (b) or a foil (c and d).

1.2 Beam transport with a foil

At first, it was difficult to propagate the beam from the foil to the target located at 1.2 meter downstream. Particles were lost on the chamber and in the best situation only 2 kA out of the 3 kA reaches the target.

We identified a position in the middle of the last drift (see foil quoted 2000 on fig. 1), that allowed to transport the whole beam intensity, but the minimum beam radius at the target was as large as 5.5 mm, i.e 3 times larger than expected without the foil. Focusing and scattering effects caused by the foil standing across the beam could not be compensated by the present solenoid lenses, whatever the tuning.

2 TRANSPORT MODEL

2.1 Beam simulation scheme

The TRAJENV code is used to simulate the propagation of the electron beam through the EOA [2-3]. Analytical expression of the magnetic field of the solenoids is taken. The boundary condition at the grounded pipe reads the following expression [4] :

$$\gamma = \gamma_0 - 2\frac{I_f}{I_0}\ln(r_p / R_{\max}) . \qquad (1)$$

Where I_f is the beam courant, r_p is pipe radius, and R_{max} is the beam radius. It is equivalent to a modified γ Lorentz factor [4].
The paraxial approximation, and the KV distribution are assumed. The space charge forces are linear. At each step Δz, between $z^{(0)}$ and next $z^{(1)}$, along the propagation axis, this slice in the (xx'yy'zz') phase space, is propagated. The transfer matrix **M** and the second order moments matrix σ are calculated to find the **X**=(x,x',y,y',z,z') vector, according to the transfer equation [5] :

$$\mathbf{X}^{(1)}=\mathbf{M}\mathbf{X}^{(0)}, \quad (2)$$

with $\sigma^{(1)}=\mathbf{M}\sigma^{(0)}\mathbf{M}^{T}$. (3)

Whether the moments matrix σ are calculated with the expression (3) for approximately linear forces, it is not anymore the case for non-linear forces.

2.2 Foil Scattering Model

The Williams scattering model is applied to the foils (foils are thin in order to consider an elastic scattering process, but thick enough to undergo a reasonable number of collisions).
The paraxial approximation is consistent with the small angle approximation of Williams theory, without transverse deviation. For each electron, the deviation angle θ^* is given by the mean squared analytical calculation [6]. The thickness of the foil is considered to be zero for the transport calculations ($\Delta z = 0$). Instead of matrix **M** in the expression (2), the scattering transfer matrix becomes

$$\mathbf{D}_{\bar{R}} = \mathbf{PRP}^{t} = \begin{bmatrix} 1 & 0 & 1 & 0 & 1 & 0 \\ 0 & \bar{\mathbf{R}}_{11} & 0 & \bar{\mathbf{R}}_{12} & 0 & \bar{\mathbf{R}}_{13} \\ 1 & 0 & 1 & 0 & 1 & 0 \\ 0 & \bar{\mathbf{R}}_{21} & 0 & \bar{\mathbf{R}}_{22} & 0 & \bar{\mathbf{R}}_{23} \\ 1 & 0 & 1 & 0 & 1 & 0 \\ 0 & 1 & 0 & 1 & 0 & 1 \end{bmatrix}, \quad (4)$$

where **P** is the passing matrix of the velocity vector from its own reference frame to the laboratory one, $\mathbf{P}^t$ is the transposed matrix of **P**, and **R** is the rotation matrix in the velocity vector frame.
A more approximated model taking into account a single tilt θ^*, allows to change the transversal angular coordinates according to the scattering transfer equation :

$$\mathbf{X}^{(1)} = \mathbf{X}^{(0)} \pm \Theta, \quad (5)$$

where $\Theta = (0, \theta^*, 0, \theta^*, 0, 0)$.
Calculation time is then reduced.

2.3 Foil Focusing Model

Fernsler *et al.* [7] explain the foil focusing effect as a result of charges and currents induced in the foil. They derived the following expression for the focal length :

$$f(r) = \frac{I_A R g_0 (1 + g_1 r^2 / R^2)}{I_b},$$

where r is the particle radius and an R the mean-squared beam radius, I_b is the beam current, I_A is the Alfven current, g_0 characterizes the lens strength and g_1 is a non-harmonic lens coefficient.
The focal length depends on the particle distribution and the parameters g_0 and g_1 are function of the ratio r_p/R, where r_p is the pipe radius. The authors give there value for three ratios and four distributions. For a KV distribution one gets :

$$f(r) = \frac{I_A R \tilde{g}_0 (r_p / R)(1 + \tilde{g}_1 (r_p / R) r^2 / R^2)}{I_b}, \quad (6)$$

with

$$\tilde{g}_0(x) = 0.5317 - 0.04650x + 0.002833x^2, \quad (7)$$

$$\tilde{g}_1(x) = 0.1067 + 0.008x - 0.0006667x^2. \quad (8)$$

One can also consider that every electron sees the mean focal length :

$$< f >= \frac{I_A R \tilde{g}_0 (1 + \tilde{g}_1)}{I_b}. \quad (10)$$

Then, we deal with another model which is slightly less accurate. In both cases the focusing transfer matrices $\mathbf{F}_f$ and $\mathbf{F}_{fm}$ can then be written as thin lens matrices.

The local focusing of a grounded foil has also been obtained by solving numerically, in an other model, the Poisson equation with beam trajectories thanks to a the PIC code M2V. On fig. 4 those trajectories, drawn with the resulting beam envelope, show the non-linear focusing effect of a foil. Each trajectory has a separate cross-over location resulting to a displacement of the overall waist. This generates a mismatching of the propagating beam.

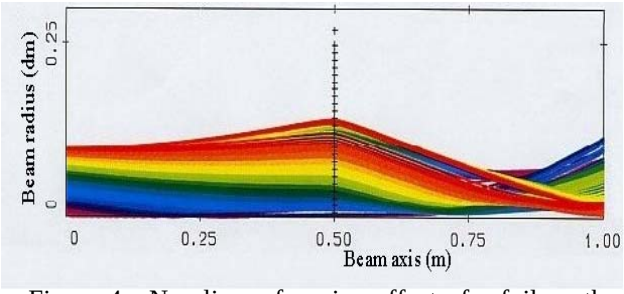

Figure 4 : Non-linear focusing effect of a foil on the beam radius in the M2V code

2.4 Overall effect of the foil

$$\mathbf{X}^{(1)} = \mathbf{F}_f \mathbf{D}_{\bar{R}} \mathbf{X}^{(0)}, \text{ first model.} \quad (11)$$

$$\mathbf{X}^{(1)} = \mathbf{F}_{fm}(\mathbf{X}^{(0)} \pm \Theta), \text{ second model} \quad (12)$$

2.5 Beam Foil second order Moments

In the first model, each moment is calculated through a quadruple integral in the phase space (xx'yy') [2]. As instance,

$$\sigma_{24}^{(1)} = \frac{\iiint x'^{(1)}(\mathbf{X}^{(0)}) y'^{(1)}(\mathbf{Y}^{(0)}) dx'^{(0)} dy'^{(0)}}{\iiint dx'^{(0)} dy'^{(0)}}. \quad (13)$$

Due to the specific initial conditions, it comes out from the simulations that the cross moments between the (xx')

and (yy') plans are negligible. Therefore, we can simply calculate the x and x' integration limits from the (xx') envelope equation. Same is done for the (yy') phase space.

In the second model [2], moments are calculated analytically :

$$\sigma_{22}^{(1)} = \sigma_{22}^{(0)} + \theta^{*2} + \frac{\sigma_{11}^{(0)}}{<f>} - 2\frac{\sigma_{12}^{(0)}}{<f>}, \quad (14)$$

$$\sigma_{44}^{(1)} = \sigma_{44}^{(0)} + \theta^{*2} + \frac{\sigma_{33}^{(0)}}{<f>} - 2\frac{\sigma_{34}^{(0)}}{<f>}, \quad (15)$$

$$\sigma_{24}^{(1)} = \sigma_{24}^{(0)} + \theta^{*2} - \frac{\sigma_{13}^{(0)}}{<f>} - \frac{\sigma_{23}^{(0)}}{<f>} - 2\frac{\sigma_{14}^{(0)}}{<f>}, \quad (16)$$

$$\sigma_{12}^{(1)} = \sigma_{12}^{(0)} - \frac{\sigma_{11}^{(0)}}{<f>}, \quad (17)$$

$$\sigma_{34}^{(1)} = \sigma_{34}^{(0)} - \frac{\sigma_{33}^{(0)}}{<f>}. \quad (18)$$

3 COMPARISON BETWEEN EXPERIMENT AND SIMULATIONS

We have compared the simulations of the beam envelope along the accelerator against the ENV code, without any foil in the EOA. The two bottom curves of the fig. 5 show only the final beam radius on the target versus solenoid #2 current. A very good agreement is obtained between the two codes ENV and TRAJENV. The two other curves represent the simulation results done with TRAJENV for the different scattering models which have been presented.

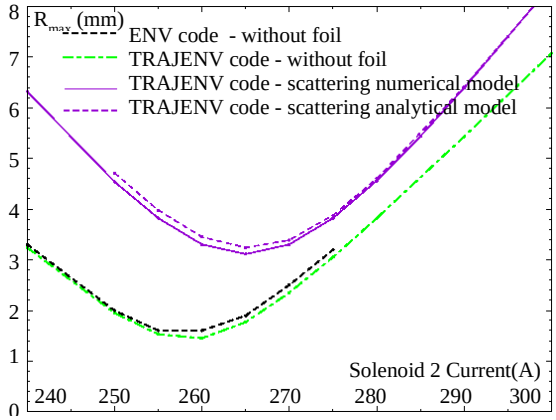

Figure 5 : Simulations with and without scattering

Several Cerenkov images of the beam on the target have been registered after the beam had crossed a 15 µm Al foil. Comparison between simulations and experimental results are presented on fig. 6 and shows very little discrepancy, validating the models used.

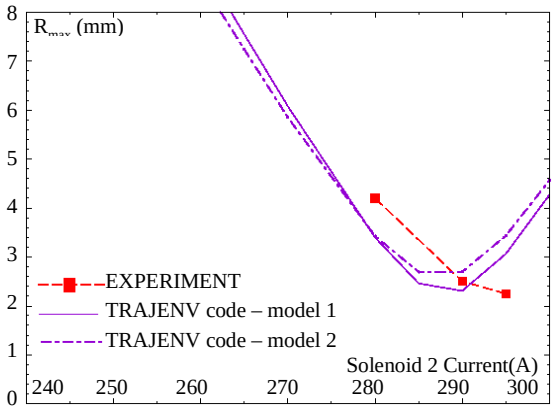

Figure 6 : Foil experiment and simulations

4 CONCLUSION

We have shown that a focalization process enhancing the Coulomb scattering phenomenon occurs when a charged particle beam goes across a thin conducting foil. The overall result is an emittance growth and a mismatching to the transport line. If no attention is paid in the design of the transport elements, the beam cannot be dealt with further. Both phenomena have to be simultaneously be taken into account for beam transport simulations. The models used here show a good agreement between simulations and experimental results. Mechanical strentgh must be calculated before decision could be made to install the device in the AIRIX accelerator [8].

5 ACKNOLEDGMENTS

We thanks J.-L. Lemaire for supporting this work and help-full discussions about physics and C. Quine for his support on M2V.

6 REFERENCES

[1] D. Guilhem, "Etude expérimentale du transport du faisceau d'électrons sur PIVAIR en présence d'une feuille anti-débris", internal communication.

[2] O. Mouton, " Effets physiques subis par un faisceau d'électrons relativistes à la traversée d'une feuille mince métallique ", Journées Accélérateurs, Roscoff, 5-7 November 2001.

[3] O. Mouton, "TRAJENV – code matriciel 2D de transport de faisceau dans un accélérateur de type AIRIX", internal communication.

[4] J. Bardy, "Code ENV – Résolution de l'équation d'enveloppe", internal communication.

[5] D. C. Carey, "The optics of charged particle beams", vol. 6, Harwood Academic Publishers, Batavia, 1987.

[6] E. J. Williams, "Multiple scattering of Fast Electrons and Alpha-Particles, and 'Curvature' of Clouds Tracks due to scattering ", Phys. Rev. 58, 1940.

[7] R. F. Fernsler, " Foil focusing electron beams ", J. Appl. Phys. 68(12), 1990.

[8] E. Merle, F. Bombardier, J. Delvaux, M. Mouillet, O. Pierret, C. Vermare, "Progress with the 2-3 kA AIRIX Electron Beam", EPAC Proceeding, Paris, 3-7 June 2002.